SUPPORTING INFORMATION

Hydrogen Bubble Templating of Fractal Ni catalysts for Water Oxidation in Alkaline Media

M. Hao[1], V. Charbonneau[1], N. N. Fomena[1], J. Gaudet[1], D. R. Bruce[2], S. Garbarino[1], D. A. Harrington[3] and D. Guay[1]*

[1] Institut national de la recherche scientifique
Énergie, matériaux et télécommunications (INRS - EMT)
1650 Lionel Boulet Blvd.
Varennes, QC Canada J3X 1S2

[2] ZincNyx Energy Solutions Inc.
8765 Ash Street – Unit 1
Vancouver, BC Canada V6P 6T3

[3] Department of Chemistry,
University of Victoria, PO Box 1700,
Victoria, BC, Canada V8W 2Y2

* Corresponding author
Email: guay@emt.inrs.ca

Table of contents

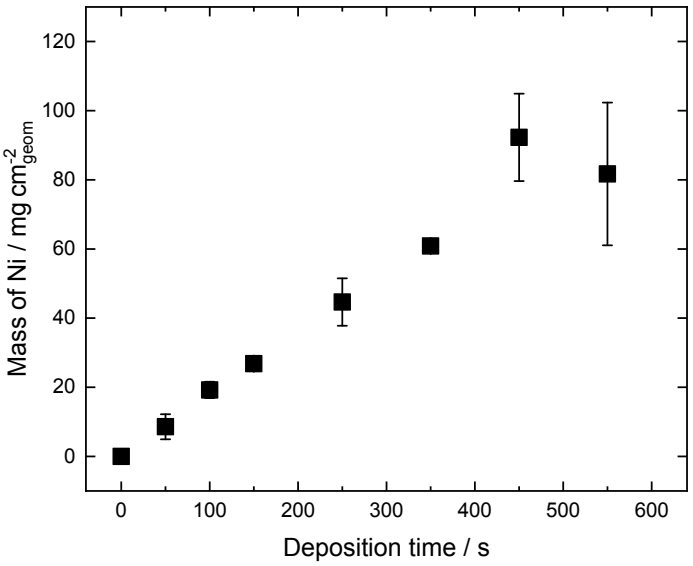

Figure S1 Effect of deposition times on the mass of Ni coatings. The substrate was a 1 cm^2 Ni plate in all cases.

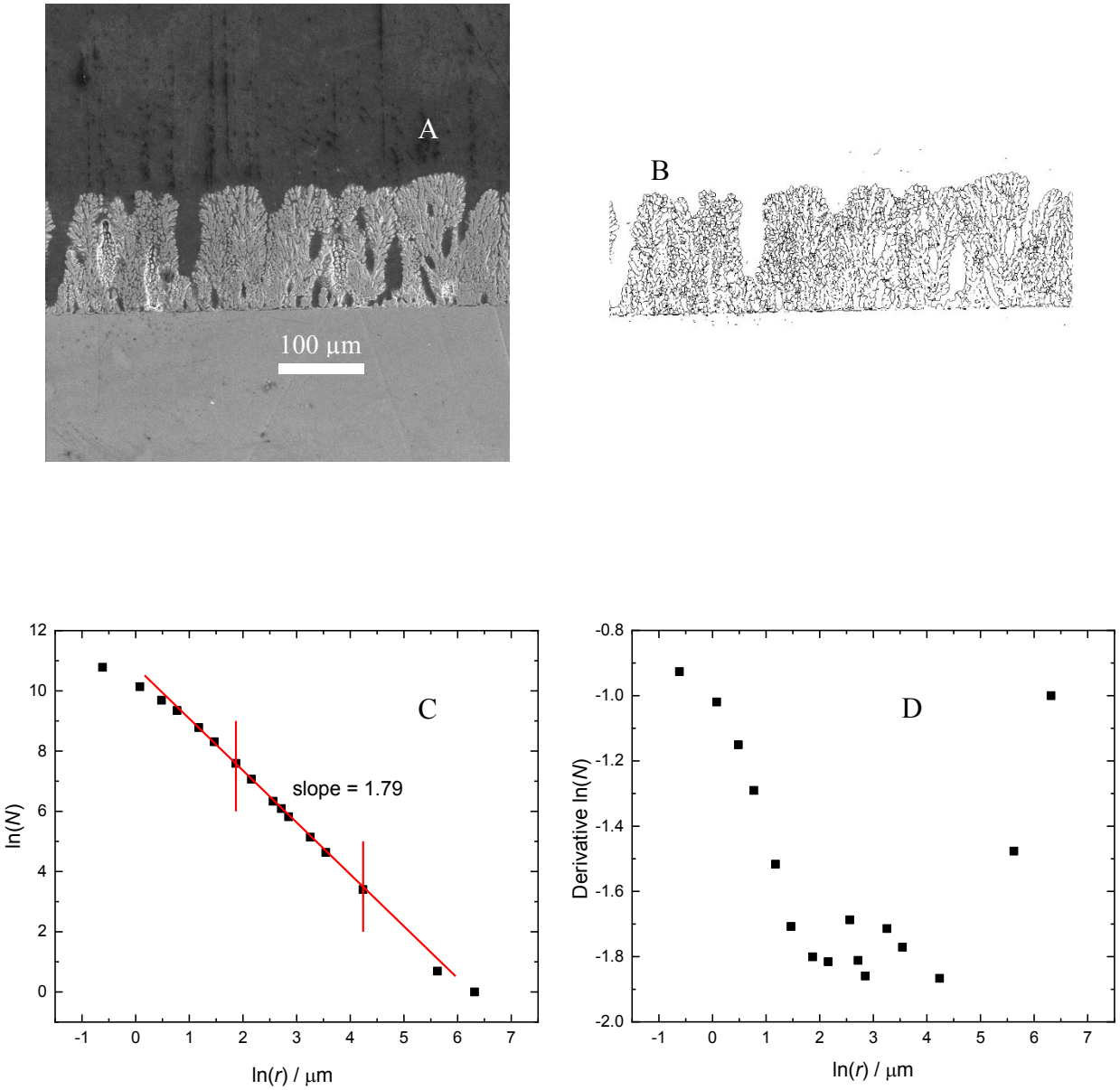

Figure S2 In (A), the original SEM cross-section image of a Ni_{DHBT} film (T_d = 450 s) at ×500 magnification. In (B), the contour image extracted from (A). In (C), ln – ln plot of box count N vs box size r. In (D), Derivative plot of ln(N) *vs* ln(r).

Fractal analysis

The SEM cross-section image of a Ni_{DHBT} sample (T_d = 450s) was taken at ×500 magnification as shown in Figure S2A. The original image was firstly converted to 8-bit grayscale

and then was segmented into features of interest and background by setting the threshold interval in-between 105 and 255. The structure's boundary was extracted by a Sobel edge detector in imagej software called ''find edge''. Then, the 2D contour image was skeletonized to one pixel wide. The final processed image is shown in Figure S2B.

The 2D contour fractal dimension was analyzed by the box counting tool in imagej. The box size was set between 1 to 1024 pixels which corresponds to a scale from 0.5 μm to 554 μm in the original image. The count of boxes containing pixels at different box sizes is presented in an ln-ln-plot (Figure S2C) of count N versus box size r. Over a certain local range of length scales the box count shows linear relationship with box size which means that porous metal materials appears to have obvious fractal characteristics. To determine the largest and the smallest size limits of the fractal behavior of the surface as well as the exact 2D fractal dimension, the derivatives of ln(N) in function of ln(r) were extracted from the ln-ln plot and is shown in Figure S2D. As a matter of fact, the derivative shows a plateau with a value of 1.79±0.05 in the interval of 6.49μm to 69.19 μm. Thus, the 2D fractal dimension D2 is estimated to be 1.79±0.05 and the upper and lower limit lengths of fractal behavior are 69.19 μm and 6.49 μm respectively. The fractal dimension D of the surface has been evaluated as $D = 2D + 1 = 2.79$. Then the value of $(L/l)^{D-2}$ mentioned in the main text is estimated to be 6.5.

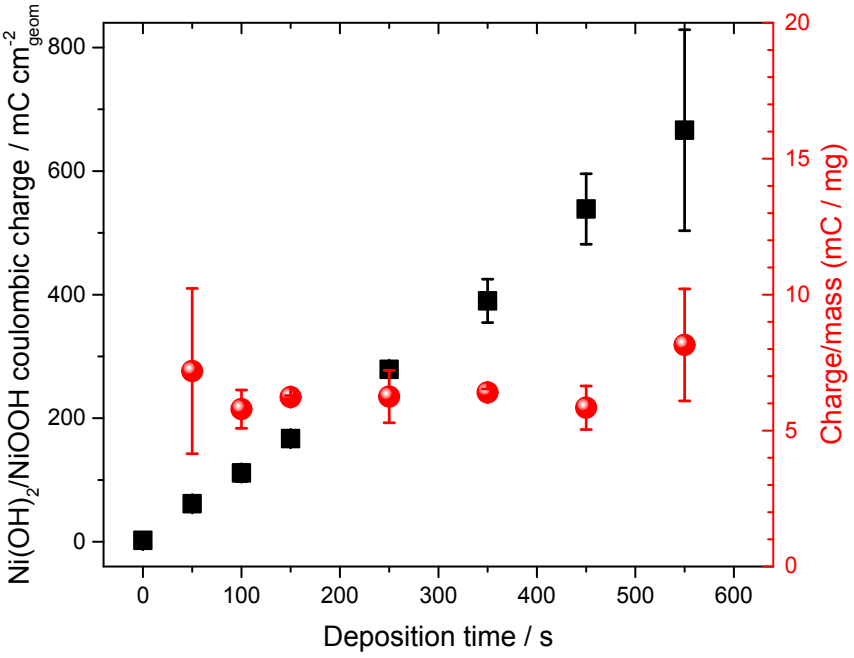

Figure S3 Effect of deposition times on the coulombic charge, Q_a, of the redox transition observed at *ca* 1.41 V, obtained from CV profiles recorded at 50 mV s^{-1} in 1 M KOH. The y-axis on the right-hand side displays the ratio between Q_a and the mass of the deposits. The fact that the Q_a / mass ratio doesn't vary with the deposition times indicates that the porous structure allows full access of the electrolyte to all the deposited material.

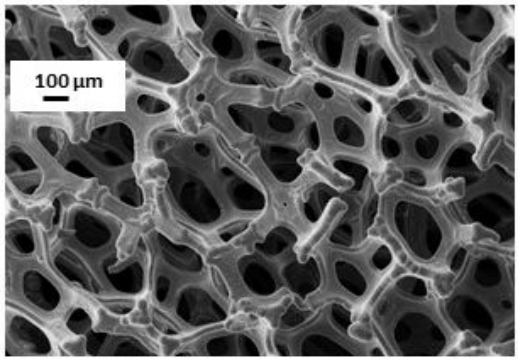

Ni foam

From ACS Appl. Mater. Interfaces 2012, 4, 3012

1cm^2 geometric → 11 cm^2 EASA

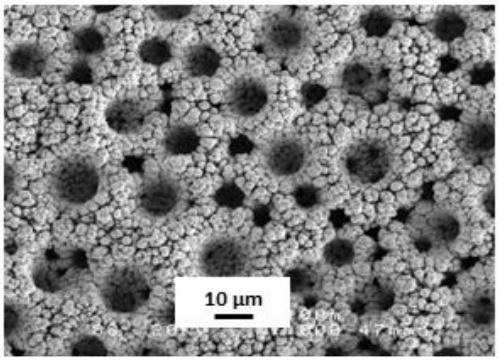

Ni_{DHBT} films

This work

1cm^2 geometric → 270 cm^2 EASA

Figure S4 SEM micrographs of Ni foam (1mm thick) and NiDHBT film.

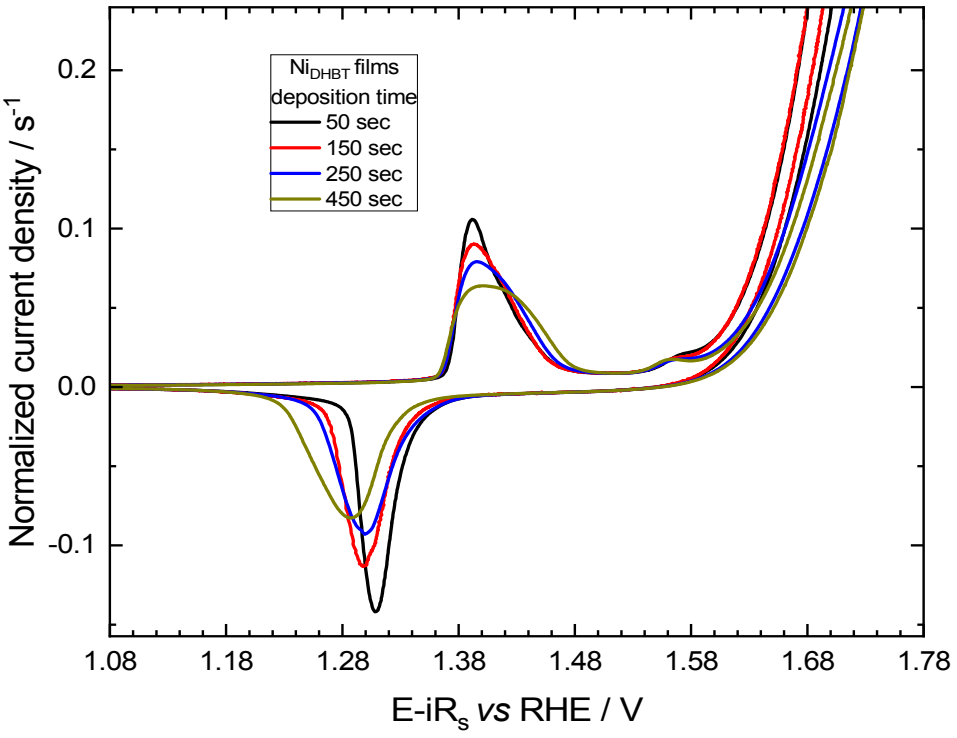

Figure S5 Normalized current density *vs* electrode potential curve. These curves were obtained following normalization of the CVs shown in Figure 2 by the corresponding Q_a values. The unit of the y-axis is thus s^{-1} and the area under the $Ni(OH)_2/Ni(OOH)$ redox transition has unit of V s^{-1}. Upon division by the scan rate (5 mV s^{-1}), the area under each $Ni(OH)_2/Ni(OOH)$ redox transition is dimensionless and has a value of 1.

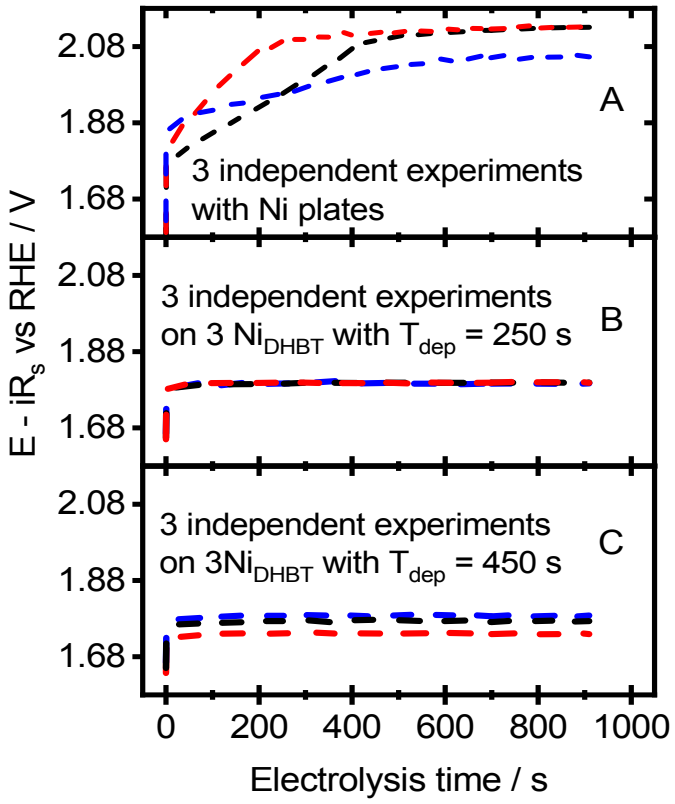

Figure S6 Chronopotentiometric curves at +250 mA cm^{-2} in 1 M KOH for different Ni plates and Ni$_{DHBT}$ electrodes; (A) Ni plates, (B) Ni$_{DHBT}$ with t_d = 250 s, and (C) Ni$_{DHBT}$ with T_d = 450 s. The error bars shown in Figure 3B were obtained from these measurements.

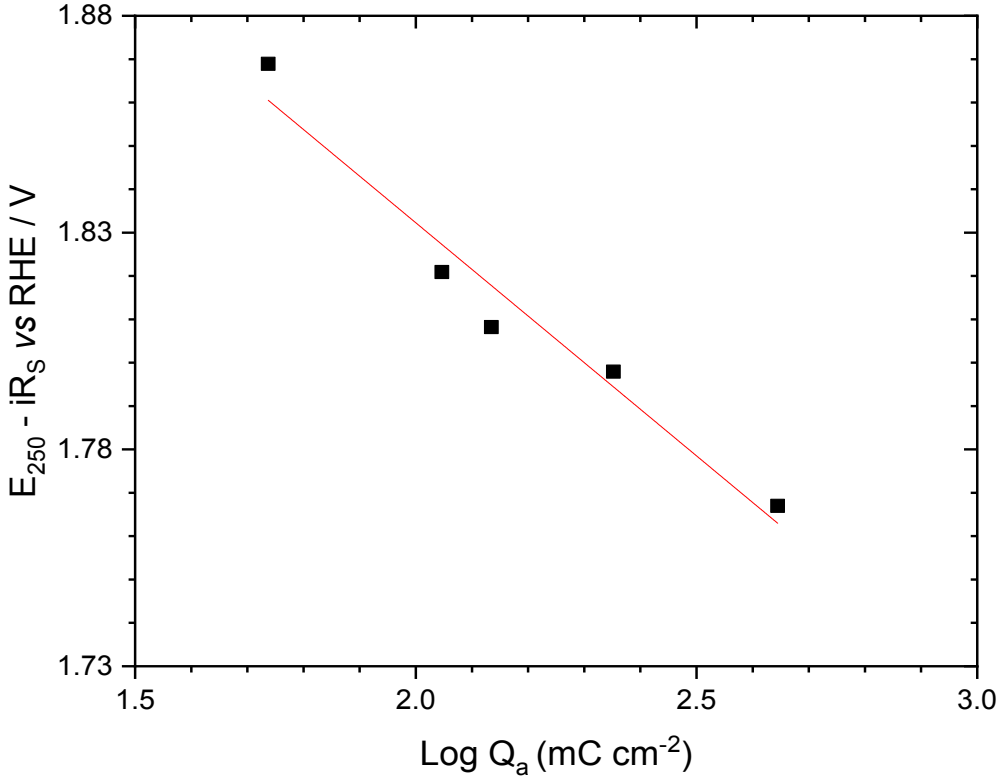

Figure S7 Variation of the IR_s-corrected electrode potential reached after 15 minutes of electrolysis at +250 mA cm^{-2} with respect to Q_a, the coulombic charge of the $Ni(OH)_2$/NiOOH transition.

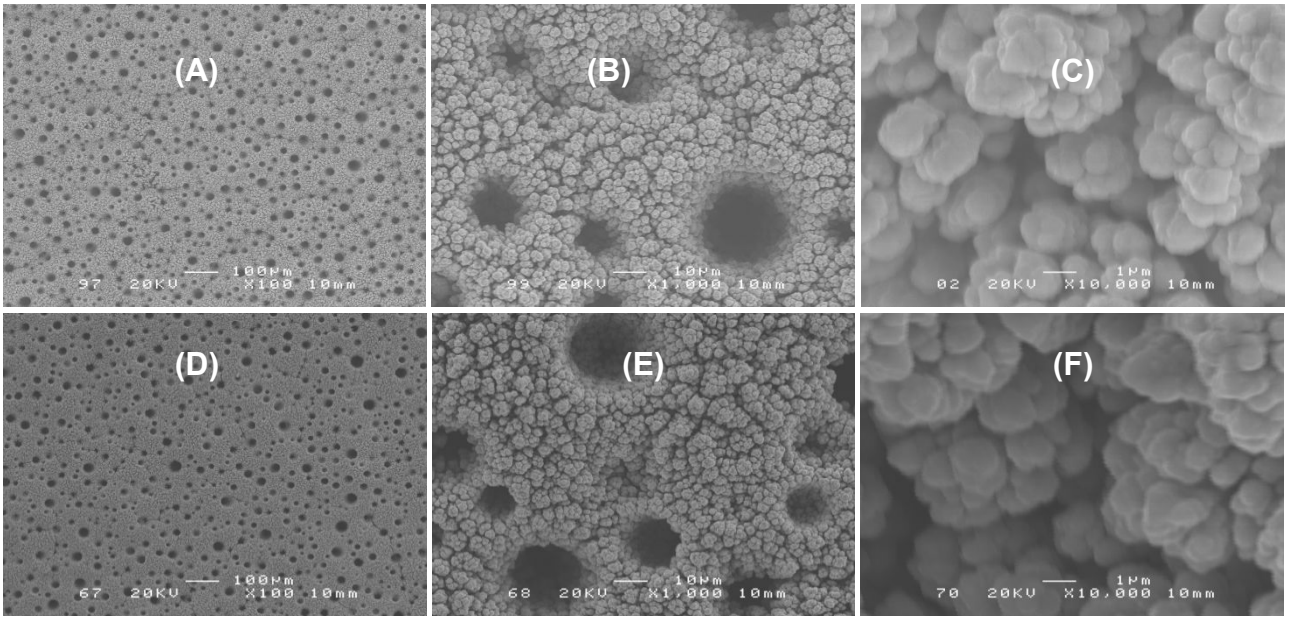

Figure S8 SEM images for Ni_{DHBT} films with T_{dep} = 450 s prior to (A, B and C) and after (D, E and F) polarization at 250 mA cm^{-2} for 15 min in 1M KOH. No morphological change due to strong O_2 gas evolution was observed.

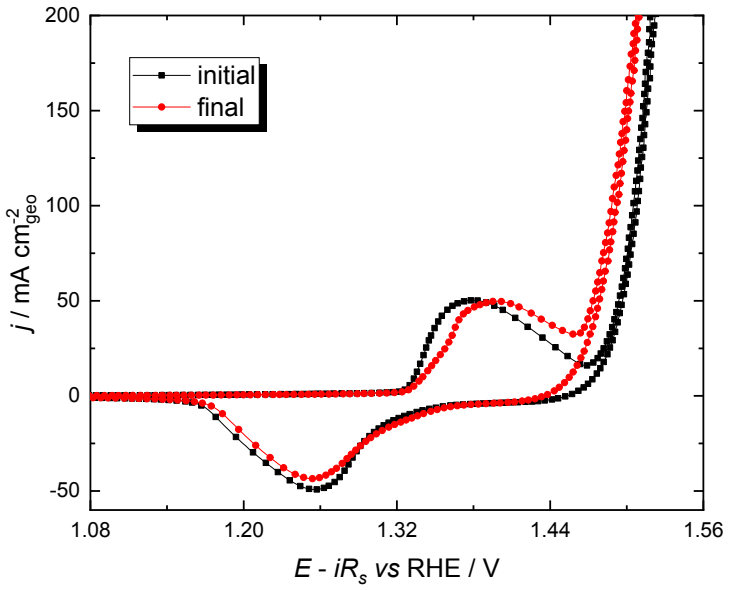

Figure S9 CVs of Ni_{DHBT} films with T_d = 450 s recorded before and after the data of Figure 5C were taken. The electrolyte was 1M KOH spiked with 10 ppm $FeCl_2$ and the CV profiles were recorded at 5 mV s^{-1}. The charge under the redox peaks centered at *ca* 1.39 V is hardly changed, although the shape of the oxidation and reduction peaks are slightly modified.